

Photometry of Three Superoutbursts of the SU UMa-type Dwarf Nova, SW Ursae Majoris

Yuichi SOEJIMA,^{1*} Daisaku NOGAMI,² Taichi KATO,¹ Makoto UEMURA,³ Akira IMADA,⁴
Kei SUGIYASU,¹ Hiroyuki MAEHARA,² Ken'ichi TORII,⁵ Kenji TANABE,⁶ Arto OKSANEN,⁷
Kazuhiro NAKAJIMA,⁸ Rudolf NOVÁK,⁹ Gianluca MASI,¹⁰ Tomáš HYNEK,¹¹ Brian MARTIN,¹²
Denis BUCZYNSKI,¹³ Elena P. PAVLENKO,¹⁴ Sergei Yu. SHUGAROV,¹⁵ Lewis M. COOK,¹⁶

¹*Department of Astronomy, Faculty of Science, Kyoto University, Sakyo-ku, Kyoto 606-8501*

**soejima@kusastro.kyoto-u.ac.jp*

²*Kwasan Observatory, Kyoto University, Yamashina-ku, Kyoto 607-8471*

³*Astrophysical Science Center, Hiroshima University, Kagamiyama, 1-3-1 Higashi-Hiroshima 739-8526*

⁴*Space Research Course in the Department of Physics, Faculty of Science,
Kagoshima University, Korimoto, Kagoshima 890-0065*

⁵*Department of Earth and Space Science, Graduate School of Science,*

Osaka University, 1-1 Machikaneyama-cho, Toyonaka, Osaka 560-0043

⁶*Department of Biosphere-Geosphere System Science, Faculty of Informatics, Okayama University of Science,
1-1 Ridai-cho, Okayama 700-0005*

⁷*Nyrola Observatory, Jyväskylä Sirius ry, Kyllikinkatu 1, FIN-40100 Jyväskylä, Finland*

⁸*VSOLJ, 124 Isatotyo, Teradani, Kumano, Mie 519-4673*

⁹*Institute of Computer Science, Faculty of Civil Engineering, Brno University of Technology, 602 00 Brno*

¹⁰*The Virtual Telescope Project, Via Madonna del Loco 47, 03023 Ceccano (FR), Italy*

¹¹*Observatory and Planetarium of Johann Palisa, VSB – Technical*

University Ostrava, Trida 17. listopadu 15, Ostrava – Poruba 708 33, Czech Republic

¹²*The King's University College; Center for Backyard Astrophysics*

(Alberta), Edmonton, Alberta, Canada T6B 2H3

¹³*Conder Brow Observatory, Littlefell Lane, Lancaster LA1 1XD, England*

¹⁴*Crimean Astrophysical Observatory, 98409, Nauchny, Crimea, Ukraine*

¹⁵*Sternberg Astronomical institute, Moscow University, Universitetsky Ave., 13, Moscow 119992, Russia, and Astronomical
Institute of Slovak Academy of Sciences, 05960, Tatranska Lomnica, Slovakia*

¹⁶*Center for Backyard Astrophysics (Concord), 1730 Helix Ct. Concord, California 94518, USA*

(Received ; accepted)

Abstract

We investigated the superhump evolution, analysing optical photometric observations of the 2000 February-March, the 2002 October-November, and the 2006 September superoutbursts of SW UMa. The superhumps evolved in the same way after their appearance during the 2000 and the 2002 superoutbursts, and probably during the 2006 one. This indicates that the superhump evolution may be governed by the invariable binary parameters. We detected a periodicity in light curve after the end of the 2000 superoutburst without phase shift, which seems to be the remains of the superhumps. We found QPOs at the end stage of the 2000 and the 2002 superoutbursts, but failed to find extraordinarily large-amplitude QPOs called ‘super-QPOs’ which previously have been observed in SW UMa.

Key words: accretion, accretion disks — stars: dwarf novae — stars: individual (SW Ursae Majoris) — stars: novae, cataclysmic variables

1. INTRODUCTION

Cataclysmic variables (CVs) are close binaries containing a white dwarf (primary) and a late-type star (secondary). The secondary fills its Roche-lobe, and transfers gas to the primary, so that if the primary star is non-magnetic, an accretion disk is formed from the material spiraling onto the white dwarf (for a review, see e.g. Warner 1995; Hellier 2001; Connors Smith 2007).

Dwarf novae are a subclass of CVs, and undergo out-

bursts which are caused by the thermal instability in the accretion disk (Osaki 1974). SU UMa-type dwarf novae are the most spectacular subgroup of the dwarf novae which are characterized by two distinct types of outbursts: more frequent normal outbursts lasting typically for a few days, and less frequent long and large-amplitude superoutbursts lasting for about two weeks. The most enigmatic feature of the superoutbursts is an occurrence of photometric light humps with an amplitude of about 0.2-0.3 mag, called “superhumps” which repeat with a few per-

cent longer period than that of the orbital motion.

Osaki (1989) has explained the general behavior of SU UMa stars by combining the thermal instability and the tidal instability. It is thus called the thermal-tidal instability model. According to this model, the disk radius is expanded at the beginning of the outburst by the increased viscosity. When an outburst pushes the outer disk beyond the critical radius for the 3:1 resonance, the tidal instability is triggered, producing a precessing eccentric disk. Superhumps can be explained as a beat phenomenon of the precession of the tidally deformed disk and the orbital motion of the system.

SW UMa is an SU UMa-type dwarf nova with a short orbital period of 81.8 min (Shafter et al. 1986), and various observations of this object were carried out so far. During the 1986 superoutburst, its superhumps were detected by Robinson et al. (1987) for the first time, and they determined the superhump period (P_{SH}) as to be 84.0 min (0.5833 days). Kato et al. (1992) found ‘super-QPOs’ with an extraordinarily large amplitude of ~ 0.2 mag and a period of ~ 6 min during the 1992 superoutburst, which is a peculiar phenomenon of the superoutbursts of SW UMa. Semeniuk et al. (1997) found that the P_{SH} was 0.05818(2) days, and the P_{SH} derivative ($P_{dot} = \dot{P}_{SH}/P_{SH}$) was 8.9×10^{-5} during the 1996 superoutburst. Nogami et al. (1998) also detected $P_{SH} = 0.05818(2)$ days, and $P_{dot} = 8.8(0.7) \times 10^{-5}$ during the same superoutburst. Nogami et al. (1998) found QPOs, but failed to detect ‘super-QPOs’. In quiescence, SW UMa is at $V = 16.5$ – 17 . A 15.9-min periodicity was discovered in its optical light curve, and also marginally detected in the soft X-ray data by *EXOSAT* (Shafter et al. 1986). This indicates that SW UMa has the nature of an intermediate polar harboring a strongly magnetized white dwarf rotating with a period of 15.9 min. Recently, Pavlenko, Shugarov, Katysheva (2000) observed the late stage of the 2000 superoutburst of SW UMa, and found late superhumps with a period of 0.1197 days and the 15.9-min oscillations.

In this paper, we analysed the photometric observations of SW UMa during the 2000, 2002, and 2006 superoutbursts. The results of the analyses are summarized in the section 3. We will discuss the properties in light curves, the superhump evolution, and QPOs in the section 4. Our conclusions are put in the last section 5.

2. OBSERVATION

We analysed the data of time-resolved CCD photometries by VSNET Collaborators. The summary of the observations is given in table 1, 2, 3, and 4. We also used the data from the AAVSO International Database and visual observations reported to VSNET for the supplement. Heliocentric corrections to the observation times, and correction for systematic differences between observers were applied before the following analysis.

Table 4. Observations during the 2006 superoutburst.

Start date*	End date*	N^\dagger	Observer ‡
3992.385	3992.518	187	M
3993.392	3993.575	207	M
3994.413	3994.582	208	M
3995.249	3995.254	10	O
3995.423	3995.428	8	M
3997.214	3997.323	502	N
3998.248	3998.312	119	O
3999.248	3999.317	124	O
3999.395	3999.598	246	M
4000.248	4000.320	185	N
4000.291	4000.334	113	P
4001.238	4001.341	344	P
4001.420	4001.558	170	M
4002.224	4002.324	378	N
4002.233	4002.318	155	O
4003.234	4003.338	102	P
4004.369	4004.458	162	M
4006.205	4006.294	45	O
4006.230	4006.316	249	N
4009.228	4009.288	171	N
4015.252	4015.332	82	O
4016.217	4016.332	111	O
4016.225	4016.331	276	N
4017.234	4017.329	230	N

* HJD-2450000.

† Number of frames.

‡ See table 1 for detail.

3. ANALYSIS AND RESULT

3.1. 2000 Superoutburst

The light curve of the 2000 February–March superoutburst is shown in figure 1. This superoutburst ignited on HJD 2451586. The magnitude reached the maximum of 10.4 mag on HJD 2451588, and successively the object faded almost constantly from HJD 2451589 to HJD 2451600. After that, the object rebrightened with an amplitude of ~ 0.1 mag on HJD 2451602. On HJD 2451605, the star entered the rapid fading phase, and for the following two weeks, there was no evidence of rebrightening outbursts which are often observed in WZ Sge-type dwarf novae and occasionally in SU UMa-type dwarf novae with a short orbital period.

We detected clear ordinary superhumps in separated two instances, from HJD 2451590 to HJD 2451597, and from HJD 2451602 to 2451605 (the left panel of figure 2). The superhump amplitude reached the first maximum of ~ 0.3 mag on HJD 2451592, and gradually declined between HJD 2451593 and 2451600. However, it regrew and reached the second maximum of ~ 0.2 mag on HJD 2451602. On HJD 2451606, at the end of rapid brightness decline of the outburst, the humps showed more complex shapes with an amplitude of ~ 0.2 mag.

After subtracting the general trend by fitting first

Table 1. Observers and instruments.

Symbol*	Telescope	CCD	Observer	Site
A	30 cm	ST-7	Kyoto Team	Japan
B	12.5 in	CB245	B. Martin	Canada
C	38 cm	SXLB	D. Buczynski	UK
D	44 cm	CB245	L. Cook	USA
E	40 cm	ST-7	R. Novák	Czech
F	38 cm	ST-7	E. Pavlenko	Ukraine
G	30 cm	electrophotometer	S. Shugarov	Russia
H	28 cm	ST-7	G. Masi	Italy
I	30 cm	ST-9	K. Tanabe	Japan
J	25 cm	AP6E	K. Torii	Japan
K	20 cm	AP7p	K. Torii	Japan
L	9 cm	ST-7	T. Hynek	Czech
M	40 cm	STL-1001E	A. Oksanen	Finland
N	25 cm	ST-7XME	H. Maehara	Japan
O	25 cm	CV04	K. Nakajima	Japan
P	40 cm	ST-7	Kyoto Team	Japan

Symbols in table 2 and 3.

Table 2. Observations during the 2000 superoutburst.

Start date*	End date*	N^\dagger	Observer [‡]	Start date*	End date*	N^\dagger	Observer [‡]
1586.950	1587.370	1261	A	1606.897	1607.148	218	A
1587.899	1588.125	493	A	1607.258	1607.275	7	G
1589.892	1590.079	803	A	1607.386	1607.502	200	C
1590.894	1591.388	1445	A	1607.292	1607.417	160	H
1591.616	1592.044	335	B	1608.283	1608.444	98	F
1591.902	1592.382	1657	A	1608.490	1608.602	193	C
1592.653	1592.902	200	B	1608.898	1609.344	726	A
1592.901	1593.164	1109	A	1609.310	1609.532	79	G
1593.685	1593.865	546	D	1609.899	1610.320	860	A
1594.367	1594.477	215	C	1610.361	1610.440	40	G
1594.900	1595.386	1524	A	1610.898	1611.345	1100	A
1595.890	1596.372	1969	A	1611.902	1612.170	522	A
1596.961	1597.379	1977	A	1612.318	1612.417	70	F
1597.893	1598.171	1422	A	1612.981	1613.080	135	A
1598.911	1599.382	936	A	1613.238	1613.267	17	F
1599.890	1600.243	1091	A	1613.903	1614.101	442	A
1601.020	1601.378	210	A	1614.403	1614.555	57	G
1602.059	1602.369	1794	A	1615.216	1615.361	67	F
1602.902	1603.298	983	A	1615.904	1616.127	552	A
1602.405	1602.399	562	E	1616.905	1617.117	536	A
1603.713	1603.967	194	B	1617.395	1617.519	63	G
1604.406	1604.531	57	G	1617.902	1618.196	723	A
1604.893	1605.278	2338	A	1618.227	1618.457	100	F
1605.954	1606.355	995	A	1619.223	1619.446	80	F
1606.279	1606.403	63	F				

* HJD-2450000.

† Number of frames.

‡ See table 1 for detail.

Table 3. Observations during the 2002 superoutburst.

Start date*	End date*	N^\dagger	Observer ‡	Start date*	End date*	N^\dagger	Observer ‡
2571.157	2571.244	425	I	2587.018	2587.325	556	K
2572.182	2572.274	506	I	2587.194	2587.321	683	I
2574.372	2574.504	93	L	2588.021	2588.333	684	K
2575.040	2575.336	312	J	2588.193	2588.285	459	I
2575.171	2575.347	1399	I	2589.038	2589.339	613	K
2576.013	2576.339	634	J	2590.074	2590.396	339	K
2576.188	2576.356	1029	I	2591.044	2591.347	372	K
2577.075	2577.338	509	J	2591.301	2591.336	23	I
2577.211	2577.354	697	I	2592.055	2592.344	575	K
2578.067	2578.329	492	J	2594.313	2594.363	96	I
2580.178	2580.295	476	I	2595.177	2595.360	980	K
2580.187	2580.346	307	J	2595.289	2595.373	79	I
2581.997	2582.337	647	K	2597.146	2597.376	500	I
2582.247	2582.354	485	I	2598.146	2598.292	442	K
2583.031	2583.351	700	K	2600.273	2600.379	131	I
2583.284	2583.355	332	I	2601.258	2601.322	40	I
2584.036	2584.339	652	K	2606.222	2606.270	101	I
2584.219	2584.333	633	I	2607.198	2607.259	82	I
2585.113	2585.328	343	K	2610.233	2610.256	40	I
2586.137	2586.342	395	K				

* HJD-2450000.

 † Number of frames. ‡ See table 1 for detail.

or second-order polynomials, we carried out the PDM method (Stellingwerf 1978) in order to measure the P_{SH} , using the data set between HJD 2451592 and HJD 2451600, from the first maximum of the superhump amplitude to before the second. From the Theta-Frequency diagram of the PDM analysis (figure 3), we determined the mean superhump frequency to be $17.213(2) \text{ day}^{-1}$ ($P_{SH} = 0.058096(6) \text{ days}$). The right panel of figure 2 shows the daily phase-averaged light curves folded by 0.058096 days, between HJD 2451590 and 2451606.

We measured the maximum times of the superhumps by eye (table 5). The cycle count (E) was set to be 1 at the first observed superhump maximum. A linear regression yields a following equation on the maximum timings:

$$HJD_{max} = 0.05818(1) \cdot E + 2451590.4914(15). \quad (1)$$

Using this equation, we drew an $O - C$ diagram for the maximum timings of the superhumps (figure 4). The $O - C$ diagram represents a decreasing trend of the P_{SH} around $E = 20$, a gradual increase of the P_{SH} in the middle (around $20 < E < 200$), and a decrease of the P_{SH} again at the end (around $E = 200$). The $O - C$ diagram between $25 < E < 203$ can be fitted by the following quadratic,

$$O - C = 2.09(9) \times 10^{-6} \cdot E^2 - 4.54(21) \times 10^{-4} \cdot E + 1.89(10) \times 10^{-2}. \quad (2)$$

From this equation, the mean P_{SH} derivative in the middle stage ($25 < E < 203$) is estimated to be $\dot{P}_{SH}/P_{SH} = 7.1(3) \times 10^{-5}$.

We applied the PDM method to the data sets at the end of this superoutburst, from HJD 2451603 to 2451606, and from HJD 2451607 to 2451610. The best estimated frequencies are $17.327(8) \text{ day}^{-1}$ for the former term and $17.248(19) \text{ day}^{-1}$, which correspond to periods of $0.05771(3)$ and $0.05798(6)$ days, respectively (figure 5, 6). Figure 7 shows the daily light curves and daily phase-averaged light curves of the end stage of this outburst (from HJD 2451603 to 2451610). The time of phase zero is the same as in figure 2, and the period used in folding is 0.0057714 days.

3.2. 2002 Superoutburst

Figure 8 shows the light curve of the 2002 October-November superoutburst. This superoutburst was detected at 11.3 mag on HJD 2452571, and the magnitude reached the maximum of 10.5 mag on HJD 2452572. The object faded almost constantly from HJD 2452575 to HJD 2452580. After the constant decline, the object rebrightened with an amplitude of ~ 0.1 mag on HJD 2452584. On HJD 2452589, this object came back to quiescence, and no rebrightening outburst was observed for following the few weeks.

Faint modulations with an amplitude of ~ 0.05 mag which are probably the seed of the superhump can be seen in the light curve on HJD 2452572, and clear superhumps were observed from HJD 2452574 to 2452588 (the left panel of figure 9). The superhump amplitude reached ~ 0.2 mag on HJD 2452574, and gradually decreased after that (between HJD 2452575 and 2452582). It, then, grew

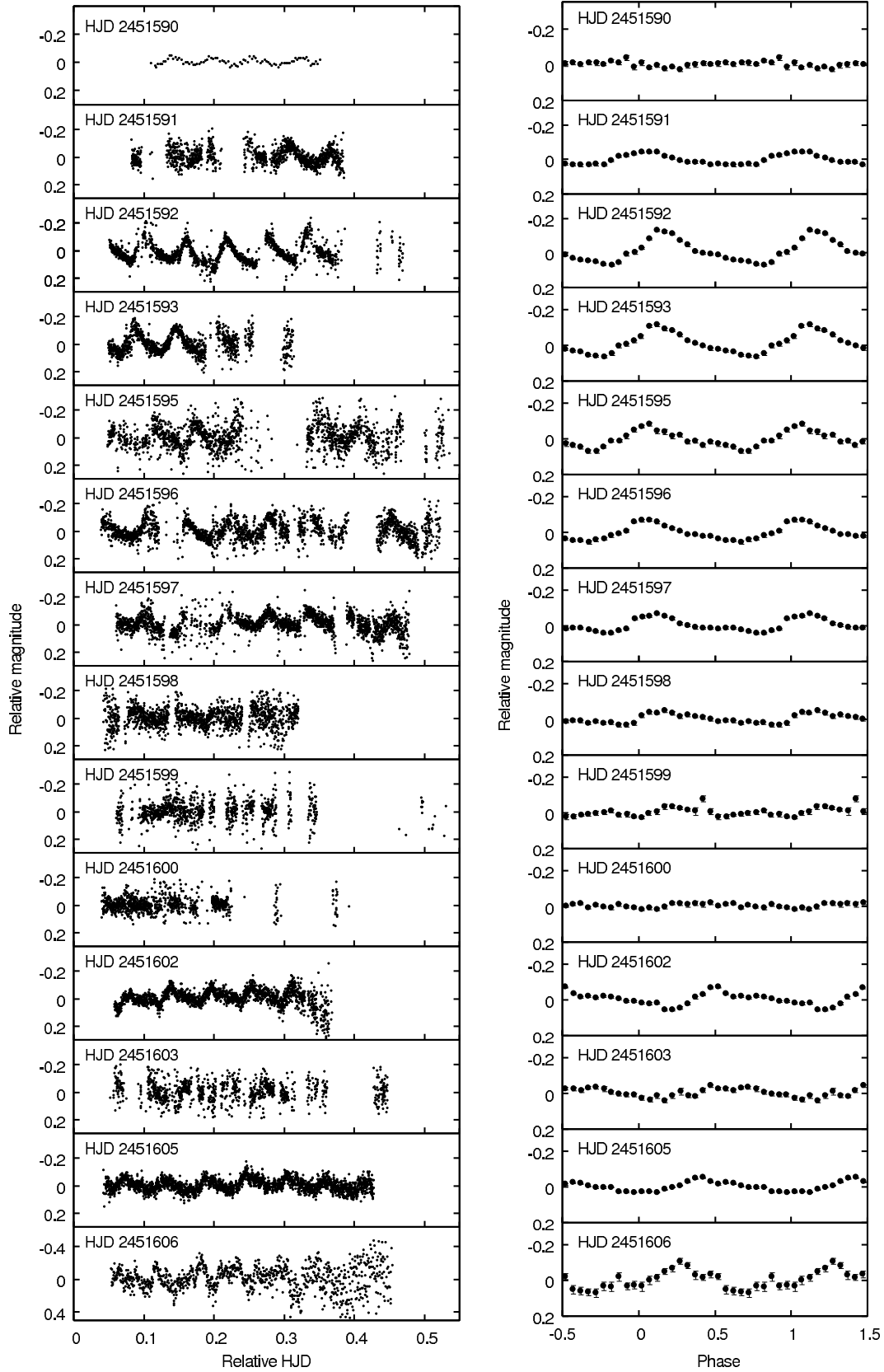


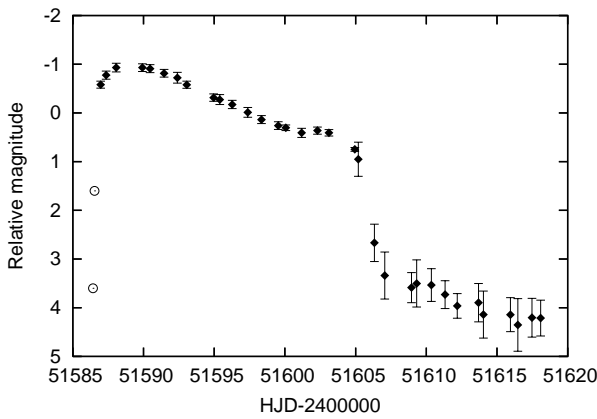
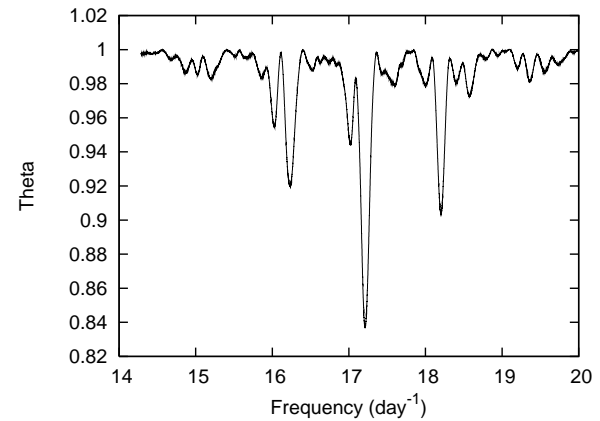
Fig. 2. Left panel: daily light curves during the 2000 superoutburst. Right panel: daily phase-averaged light curves of the 2000 superoutburst folded by 0.058096 days.

Table 5. Timings of the superhump maxima of the 2000 superoutburst.

E^*	HJD-2400000	$O - C^\dagger$ (days)	E^*	HJD-2400000	$O - C^\dagger$ (days)
1	51590.54104	-0.0078	95	51596.01289	-0.0064
2	51590.59543	-0.0116	100	51596.30185	-0.0084
3	51590.65317	-0.0120	112	51597.00305	-0.0056
4	51590.72575	0.0023	114	51597.12182	-0.0032
14	51591.31082	0.0054	115	51597.18023	-0.0030
15	51591.36996	0.0063	116	51597.23699	-0.0044
25	51591.95155	0.0059	199	51602.08108	0.0093
26	51592.01357	0.0098	200	51602.13994	0.0099
27	51592.07032	0.0083	201	51602.19721	0.0090
28	51592.13068	0.0105	202	51602.25615	0.0098
29	51592.18715	0.0088	203	51602.31676	0.0122
38	51592.70628	0.0041	248	51604.92115	-0.0022
39	51592.76541	0.0051	249	51604.98156	-0.0000
40	51592.82119	0.0026	250	51605.04197	0.0021
41	51592.88033	0.0036	251	51605.10237	0.0043
42	51592.93946	0.0045	252	51605.16034	0.0041
43	51592.99860	0.0055	253	51605.21166	-0.0027
44	51593.05774	0.0064	255	51605.32847	-0.0022
76	51594.90930	-0.0042	256	51605.38403	-0.0049
77	51594.96777	-0.0040	257	51605.44176	-0.0053
78	51595.02425	-0.0057	258	51605.50102	-0.0043
83	51595.31579	-0.0051	259	51605.56151	-0.0020
84	51595.37235	-0.0068	260	51605.61852	-0.0032
85	51595.43109	-0.0062	266	51605.96612	-0.0022
86	51595.48982	-0.0057	237	51606.01914	-0.0074
87	51595.54838	-0.0053	268	51606.08339	-0.0013
88	51595.60611	-0.0058	269	51606.13716	-0.0111
89	51595.66384	-0.0062	270	51606.19748	-0.0036
94	51595.95572	-0.0054	271	51606.24902	-0.0102

* Cycle count.

† Using equation (1).

**Fig. 1.** Light curve of the 2000 February-March superoutburst. The abscissa is HJD, and the ordinate is the relative magnitude to a comparison star. The filled diamonds are average magnitudes of the CCD observations, and the bars represent the dispersion calculated by using data on each day. The open circles represent visual observations.**Fig. 3.** Theta-Frequency diagram obtained by the PDM analysis from the data of the middle stage of the superhumps during the 2000 superoutburst, between HJD 2451592 and 2451600.

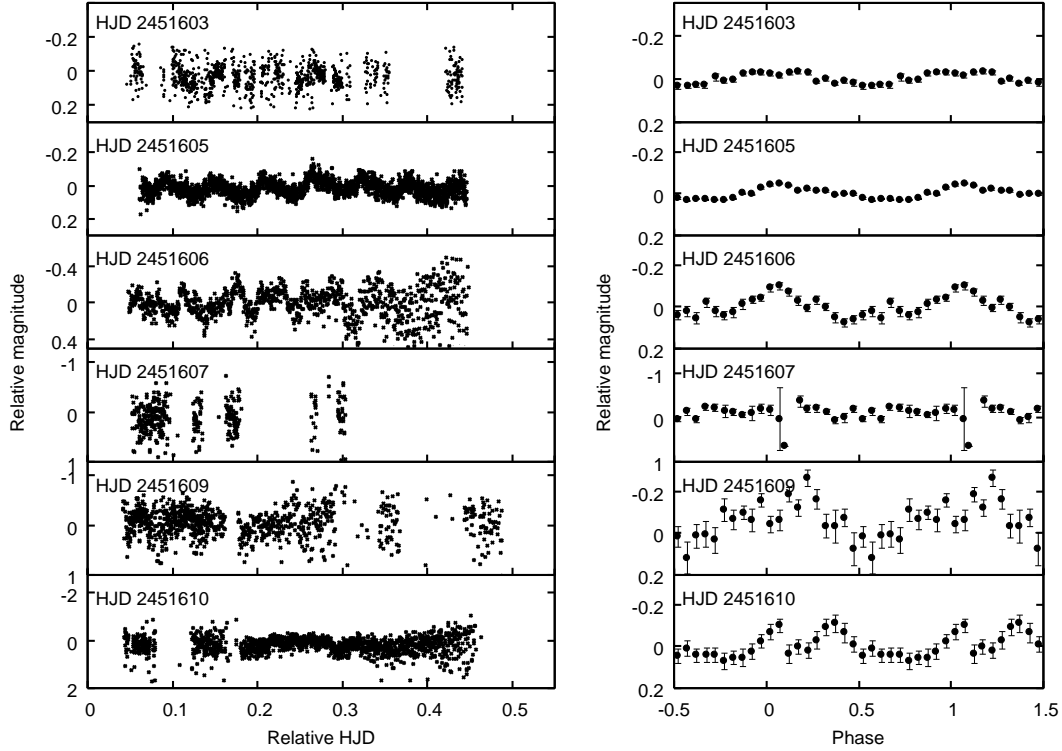


Fig. 7. Left panel: daily light curves at and after the end stage of the 2000 superoutburst. Right panel: daily phase-averaged light curves folded by 0.05771 days.

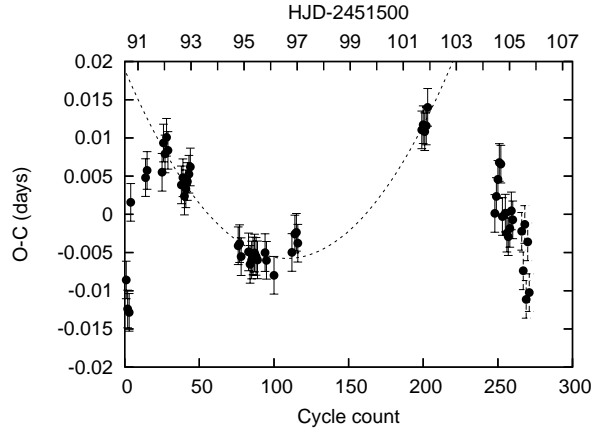


Fig. 4. $O - C$ diagram of the superhump maximum timings of the 2000 superoutburst listed in table 5. The curved line is obtained by a quadratic polynomial fitting to the $O - C$ (equation (2)).

up again around HJD 2452584. There are obscure humps with an amplitude of ~ 0.5 mag in the light curve of HJD 2452589, near the quiescence level.

We determined the average superhump frequency to be $17.161(2) \text{ day}^{-1}$ ($P_{SH} = 0.058271(5)$ days) by applying the PDM method to data between HJD 2452574 and 2452582, from the first amplitude maximum to before the second (figure 10). The right panel of figure 9 represents the daily phase-averaged light curves folded by 0.058271 days from HJD 2452572 to 2452588.

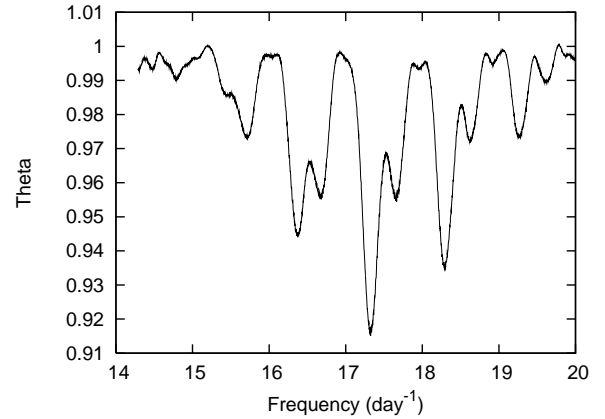


Fig. 5. Theta-Frequency diagram obtained by the PDM analysis from the data of the end stage of the 2000 superoutburst, between HJD 2451603 and 2451606.

We measured the maximum times of the superhumps by eye (table 6). A linear regression yields the following equation:

$$HJD_{max} = 0.05826(1) \cdot E + 2452574.3454(15). \quad (3)$$

Using equation 3, we obtained an $O - C$ diagram for the timings of the superhump maxima of this superoutburst (figure 11). Figure 11 indicates that the P_{SH} decreased around $E = 10$, and gradually increased around $10 < E < 150$, and, subsequently, decreased again around $E = 150$. For $12 < E < 153$, the best fitting quadratic equation is

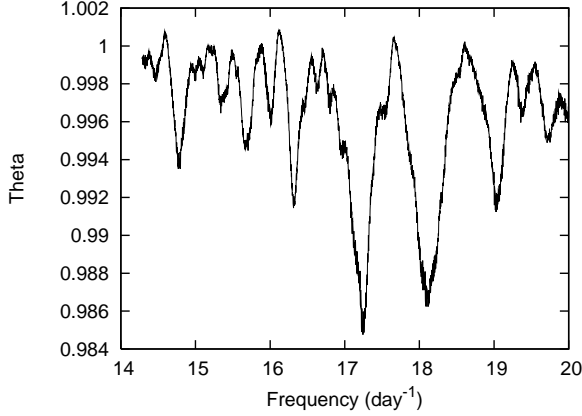


Fig. 6. Theta-Frequency diagram obtained by the PDM analysis from the data after the 2000 superoutburst, between HJD 2451607 and 2451610.

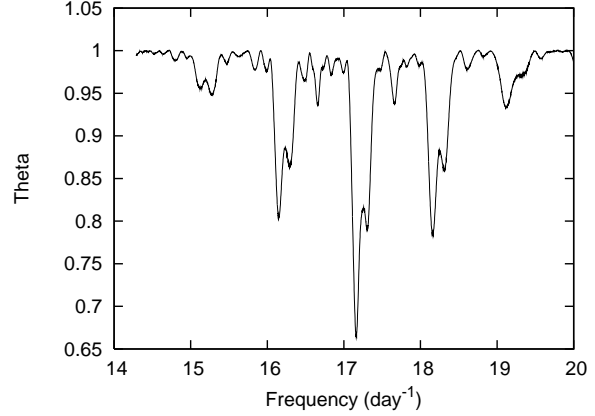


Fig. 10. Theta-Frequency diagram obtained by the PDM analysis from the data of the middle stage of the superhumps during the 2002 superoutburst, between HJD 2452574 and 2452582.

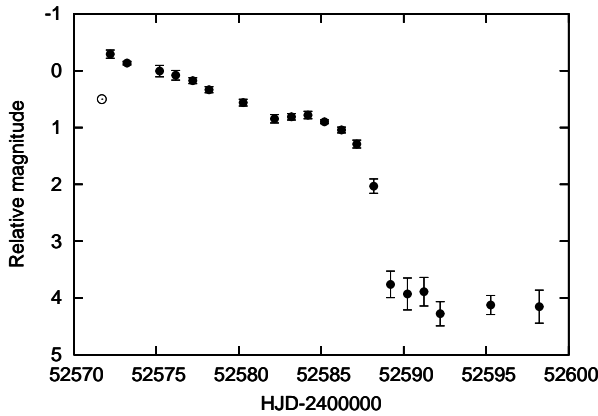


Fig. 8. Light curve of the 2002 October-November superoutburst. The abscissa is HJD, and the ordinate is the relative magnitude to a comparison star. The filled diamonds are average magnitudes of the CCD observations and the bars represent the dispersion calculated by using data on each day. The open circle represents a visual observation.

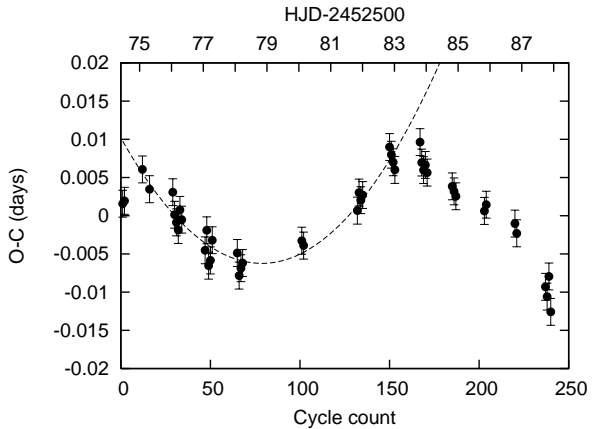


Fig. 11. $O - C$ diagram of the superhump maximum timings of the 2002 superoutburst listed in table 6. The curved line is obtained by a quadratic polynomial fitting to the $O - C$ (equation (4)).

given by:

$$O - C = 2.65(18) \times 10^{-6} \cdot E^2 - 4.18(33) \times 10^{-4} \cdot E + 1.02(12) \times 10^{-2}. \quad (4)$$

From this equation, the mean P_{SH} derivative for $12 < E < 153$ is estimated to be $P_{dot} = 9.1(6) \times 10^{-5}$.

Using the data set after the rapid decline phase (HJD 2452589 and 2452592), we carried out the PDM analysis. No plausible frequency was detected, however (figure 12).

3.3. 2006 Superoutburst

The light curve of the 2006 September superoutburst is shown in figure 13. This superoutburst started on HJD 2453991, and the magnitude became a maximum of 10.3 mag on HJD 245392. This object also showed a rebrightening at the late stage of this outburst (around HJD 2454009) as in the 2000 and the 2002 one.

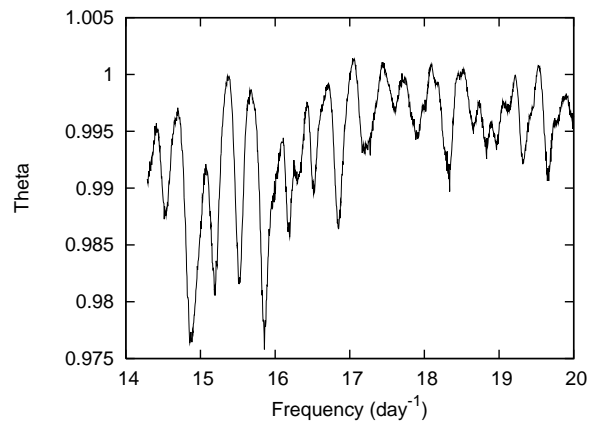


Fig. 12. Theta-Frequency diagram obtained by the PDM analysis from the data after the plateau phase of the 2002 superoutburst between HJD 2452589 and 2452592.

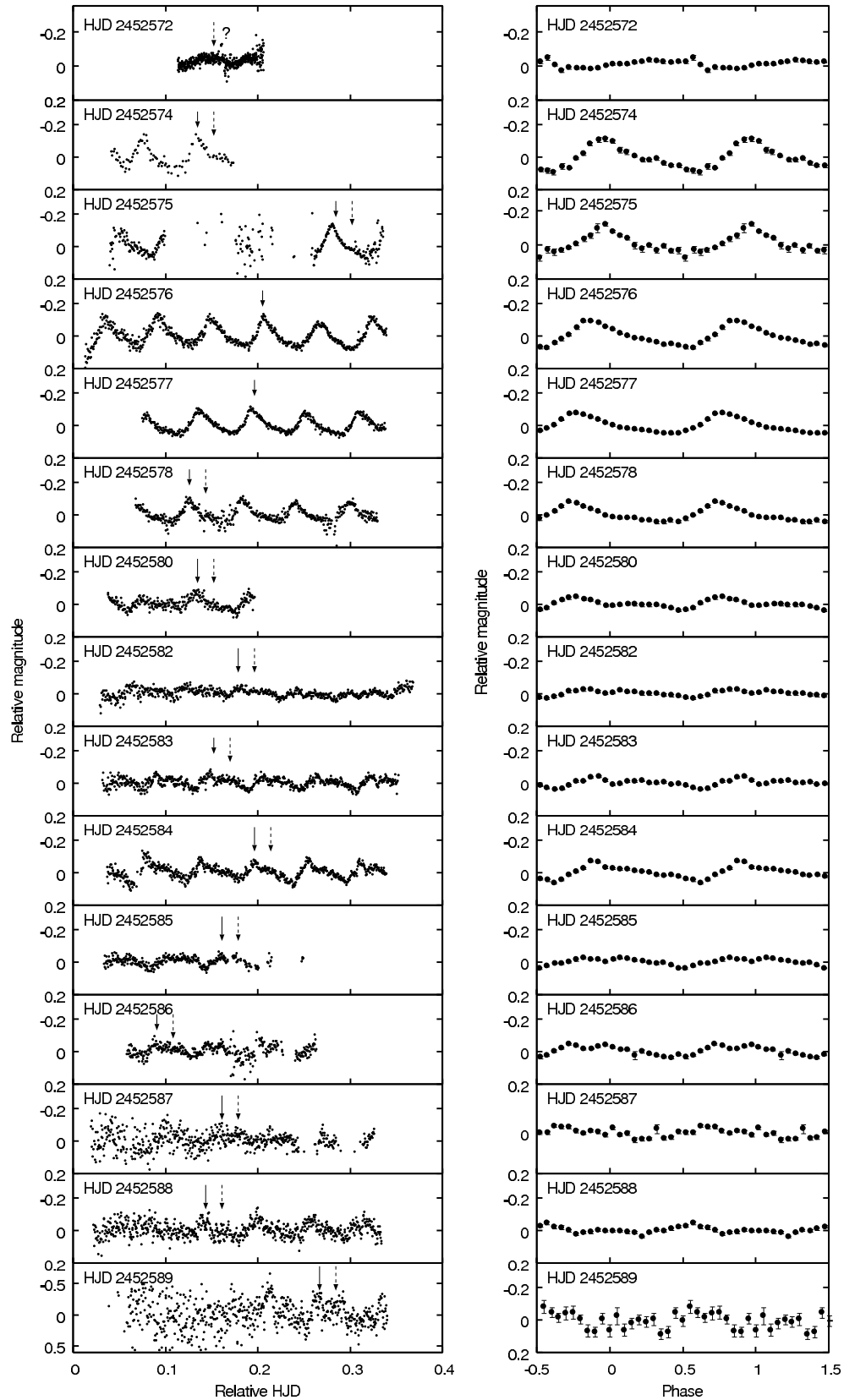


Fig. 9. Left panel: daily light curves during the 2002 superoutburst. The solid arrows and the dashed arrows indicate positions of two kinds of humps, respectively (see section 4.3 in detail). Right panel: daily phase-averaged light curves folded by 0.058278 days.

Table 6. Timings of the superhump maxima of the 2002 superoutburst.

E^*	HJD-2400000	$O - C^\dagger$ (days)	E^*	HJD-2400000	$O - C^\dagger$ (days)
1	52574.40521	0.0041	134	52582.15419	0.0021
2	52574.46385	0.0044	135	52582.21313	0.0028
12	52575.05056	0.0064	150	52583.09330	0.0090
16	52575.28101	0.0038	151	52583.15056	0.0080
29	52576.03799	0.0033	152	52583.20782	0.0070
30	52576.09330	0.0004	153	52583.26508	0.0060
31	52576.15056	-0.0006	167	52584.08436	0.0096
32	52576.20782	-0.0016	168	52584.13994	0.0070
33	52576.26871	0.0010	169	52584.19721	0.0060
34	52576.32570	-0.0003	170	52584.25614	0.0066
47	52577.07905	-0.0043	171	52584.31341	0.0056
48	52577.13994	-0.0017	185	52585.12723	0.0038
49	52577.19357	-0.0063	186	52585.18485	0.0032
50	52577.25251	-0.0056	187	52585.24246	0.0025
51	52577.31341	-0.0030	203	52586.17270	0.0006
65	52578.12737	-0.0047	204	52586.23177	0.0014
66	52578.18268	-0.0076	220	52587.16145	-0.0011
67	52578.24190	-0.0067	221	52587.21844	-0.0024
68	52578.30084	-0.0060	237	52588.14358	-0.0094
101	52580.22633	-0.0031	238	52588.20056	-0.0107
102	52580.28394	-0.0038	239	52588.26145	-0.0081
132	52582.03631	0.0007	240	52588.31508	-0.0127
133	52582.09693	0.0031			

* Cycle count.

† Using equation (3).

Clear superhumps have been observed between HJD 2453997 and 2454009 (the left panel of figure 14). The superhump amplitude was increasing until HJD 2454000, and decreasing thereafter. Figure 15 shows the Theta-Frequency diagram of the PDM analysis of the data between HJD 2454000 and 2454009. After the first amplitude maximum, we determined the most probable superhump frequency to be $17.226(3) \text{ day}^{-1}$ ($P_{SH} = 0.058050(10) \text{ days}$). The daily phase-averaged light curves folded by 0.058050 days between HJD 2453997 and 2454009 are exhibited in the right panel of figure 14.

We measured the maximum times of the superhumps by eye (table 7). A linear regression yields a following equation on the maximum timings:

$$HJD_{max} = 0.05816(3) \cdot E + 2453997.6109(26). \quad (5)$$

We calculated the $O - C$ values of the maximum timings of the superhumps, based on equation 5, and plotted them on figure 16. This figure shows a decreasing trend of the P_{SH} around $E = 30$, and a gradual increase around $E > 40$. The $O - C$ diagram between $46 < E < 200$ can be fitted by the following quadratic,

$$O - C = 1.89(18) \times 10^{-6} \cdot E^2 - 4.40(42) \times 10^{-4} \cdot E + 2.10(23) \times 10^{-2}. \quad (6)$$

This equation yields the mean P_{SH} derivative for $46 < E < 200$, $P_{dot} = 6.5(0.6) \times 10^{-5}$.

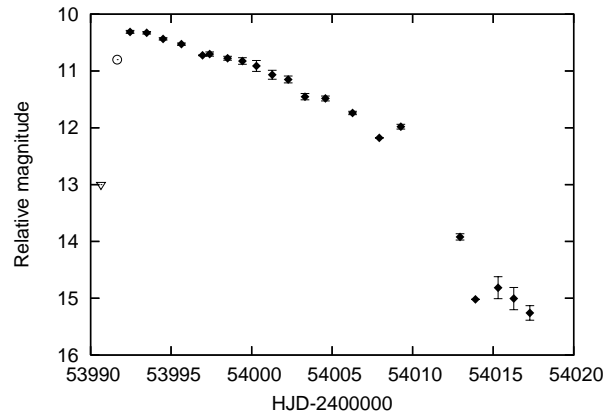


Fig. 13. Light curve of the 2006 September superoutburst. The abscissa is HJD, and the ordinate is the relative magnitude to a comparison star. The filled diamonds are average magnitudes of the CCD observations and the bars represent the dispersion calculated by using data on each day. The open circles and the bottom triangle mean the visual and the upper limit, respectively.

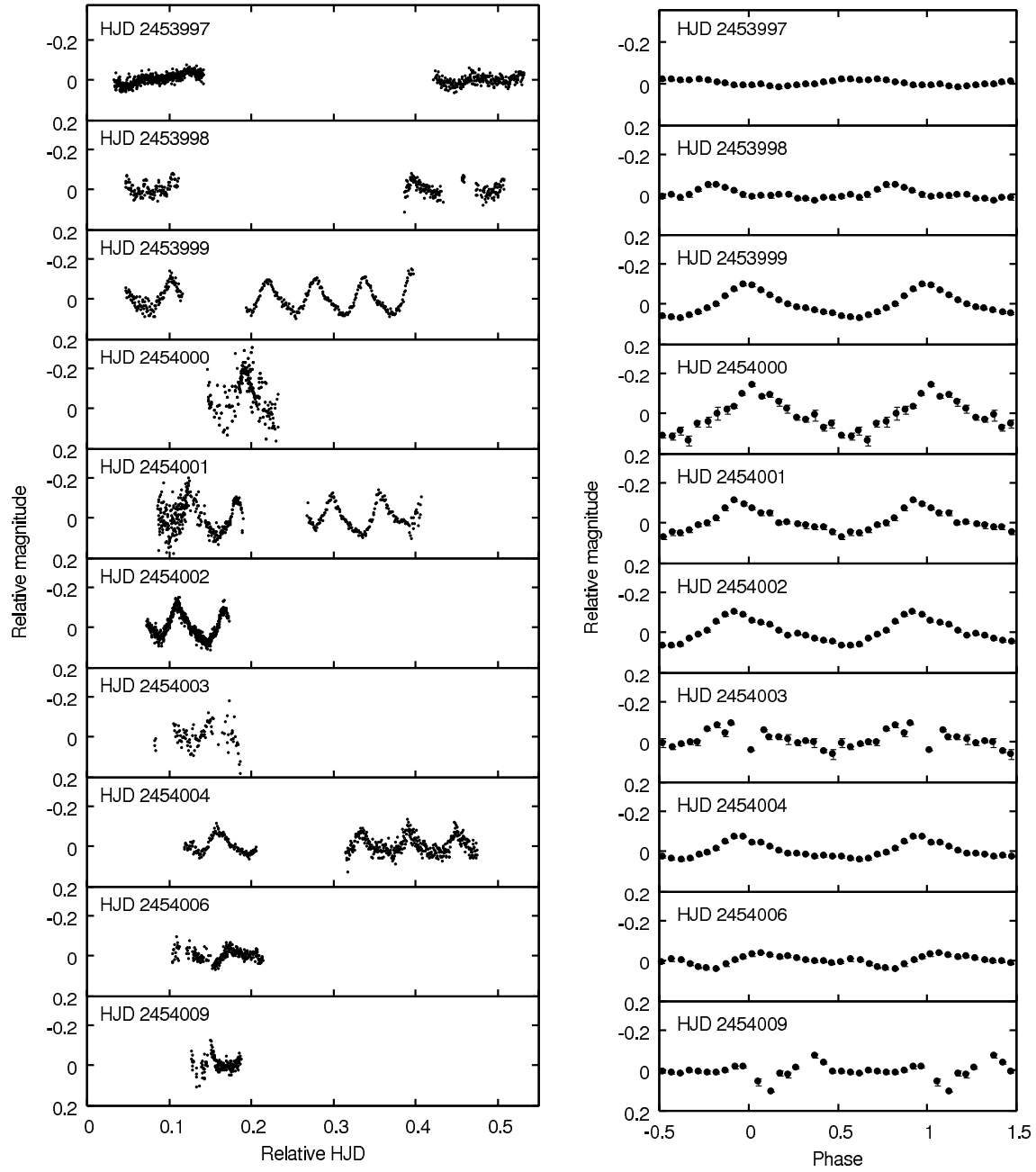


Fig. 14. Left panel: daily light curves during the 2006 superoutburst. Right panel: daily phase-averaged light curves folded by 0.058063 days.

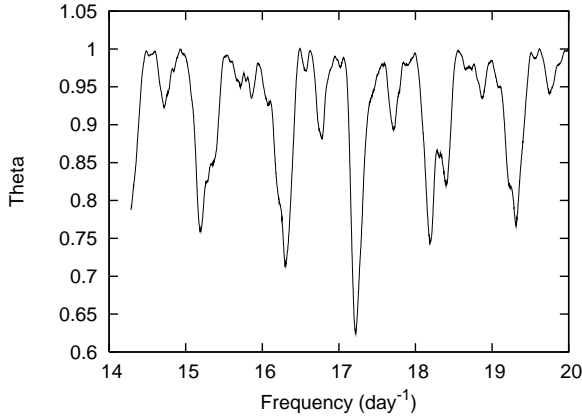


Fig. 15. Theta-Frequency diagram obtained by the PDM analysis from the data of the middle stage of the superhumps during the 2006 superoutburst, between HJD 2454000 and 2454009.

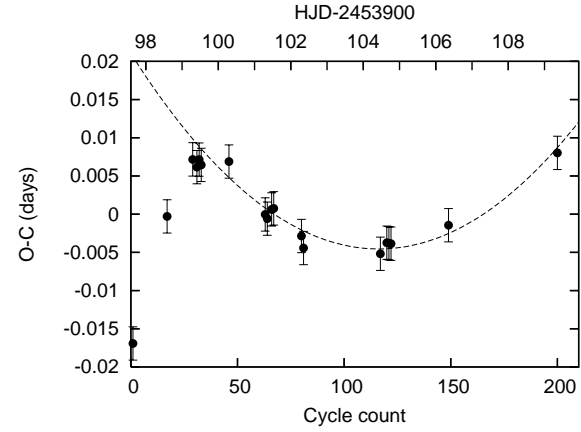


Fig. 16. $O - C$ diagram of the superhump maximum timings of the 2006 superoutburst listed in table 7. The curved line is obtained by a quadratic polynomial fitting to the $O - C$ (equation (6)).

Table 7. Timings of superhump maxima of the 2006 superoutburst.

E^*	HJD-2400000	$O - C^\dagger$ (days)
1	53997.65210	-0.01642
17	53998.59922	0.00044
29	53999.30454	0.00806
31	53999.41984	0.00708
32	53999.47898	0.00808
33	53999.53643	0.00739
46	54000.29290	0.00803
63	54001.27460	0.00133
64	54001.33221	0.00080
66	54001.44670	0.00203
67	54001.50590	0.00218
80	54002.26043	-0.00124
81	54002.31700	-0.00281
117	54004.41090	-0.00305
120	54004.58660	-0.00157
121	54004.64360	-0.00162
122	54004.70120	-0.00168
149	54006.27453	0.00112
200	54009.24991	0.01131

* Cycle count.

† Using equation (5).

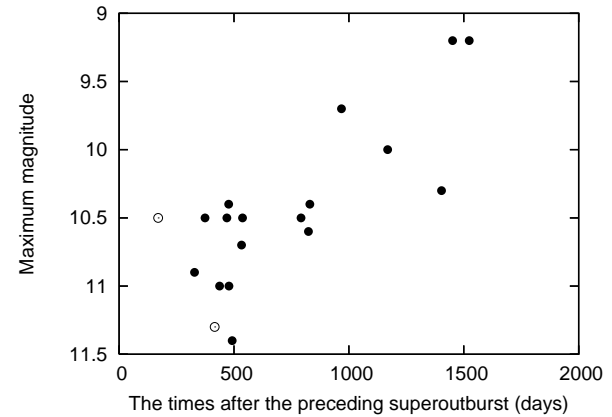


Fig. 18. The relation between the maximum magnitude of an outburst and the time after the preceding superoutburst of SW UMa. The filled circles and the open circles represent superoutbursts, and normal outbursts, respectively.

3.4. Outbursts of SW UMa

Figure 17 exhibits the long-term light curve of SW UMa, constructed from enormous number of visual observations reported to AAVSO in the past 40 years. We investigated the duration and maximum magnitude of each outburst using VSNET, AAVSO, and AFOEV archival data (table 8), and checked them against previous works (table 1 in Wenzel & Richter 1986, table 4 in Howell et al. 1995). Most outbursts of SW UMa are a superoutburst, but the 1976 and the 1993 February outbursts are the only two certain normal outbursts, judging from their durations. A single observation of $V = 12.2$ on HJD 2443152 was reported to AFOEV, which seems an outburst, but can not be classified because of the lack of observations. Figure 18 shows the relation between the maximum magnitude of an outburst and the time after the preceding superoutburst.

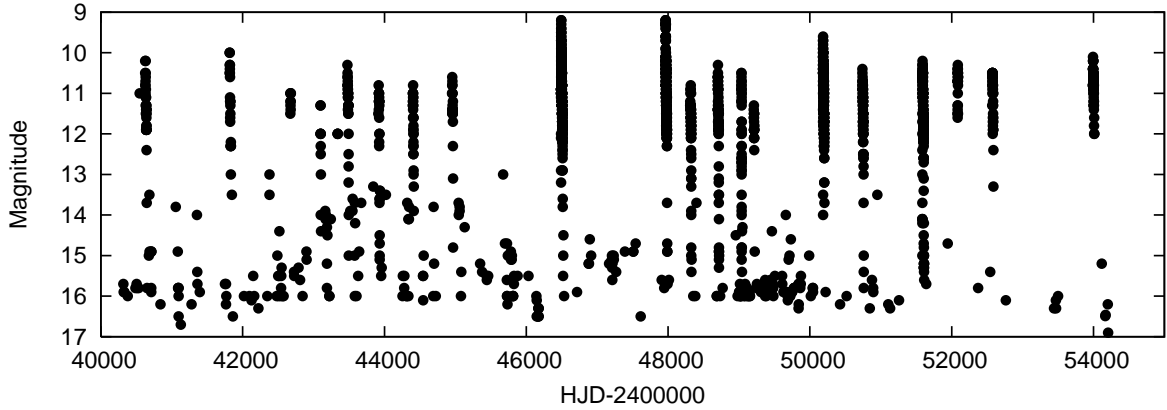


Fig. 17. Long-term light curve of SW UMa. The abscissa is HJD, and the ordinate is magnitude. The filled circles represent visual observations.

Table 8. Properties of outbursts.

Year	Start Date*	End Date*	Duration (days) [†]	m_{max}^{\ddagger}
1970	40624	40645	22	10.2
1973	41814-41816	41834	19-21	10.0
1975	42662-42663	42679-42682	17-21	10.6
1976 [§]	43098	43100	3	11.3
1977 Jan.	HJD 2443152 (single obs.)			12.2
1977 Dec.	43474-43478	43494	17-21	10.5
1979	43917	43930	14	10.8
1980	44396-44400	44412	13-17	11.0
1981	44945-44953	44967	15-23	10.7
1986	46491	46513	23	9.2
1990	47964	47985	22	9.2
1991	48313	48327	15	10.9
1992	48701	48716	17	10.5
1993 Feb. [§]	49035	49038	4	10.5
1993 Aug.	49208	49217	10	11.4
1996	50185	50203	19	9.7
1997	50740	50756	17	10.5
2000	51586	51605	20	10.4
2001	52082	52090-52098	9-17	10.4
2002	52571	52588	18	10.5
2006	53991	54012	23	10.3

* HJD-2400000.

[†] Days of $V \geq 13$.

[‡] Maximum magnitude of the outburst.

[§] Normal outburst.

3.5. QPOs

After subtracting the mean superhump profile, we constructed power spectra of each day during the 2000, the 2002, and the 2006 superoutbursts in order to detect QPOs. The left panels in figure 19 are the power spectra from the data of HJD 2451605 and 2452587, and the strongest signals correspond to 11.3 min and 10.6 min, respectively. The right panels in figure 19 represent the phase-averaged light curves folded by the best estimated period.

4. DISCUSSION

4.1. Light Curve Properties

During three superoutbursts we investigated, the brightness decline was slowed down when the superhumps developed (see figures, 1, 2, 8, 9, 13, and 14). Especially, there was a slight rebrightening at the same time when the regrowth of the superhump amplitude occurred during the 2000 and the 2002 superoutbursts. Since the emitted energy during an outburst is essentially given by the amount of mass accreted inward, this phenomenon indicates the regrowth of disk eccentricity and the resurgence of inward flow of material caused by the tidal torque in the accretion disk at the end stage of these outbursts. In the case of the 2006 superoutburst, although a rebrightening was observed at the end end stage of the outburst (HJD 2454009), we can trace the variation of the superhump amplitude due to the lack of the observation (figure 13). A regrowth of the superhump would have occurred during this superoutburst as the previous two superoutbursts.

Some SU UMa-type dwarf novae, e.g. SW UMa (Howell et al. 1995) and WX Cet (Kato 1995, Sterken et al. 2007), show more various scales of superoutbursts than ordinary SU UMa-type dwarf novae. Osaki (1995) indicated that if \dot{M} is considered to be constant, the amplitude of a superoutburst is proportional to t_{wait-S} , where \dot{M} is the mass transfer rate from the secondary, and t_{wait-S} is the waiting time for the next superoutburst after which any normal outburst can trigger a superoutburst. Figure 18 shows that the maximum magnitude of a superoutburst has roughly linear correlation with the time after the preceding superoutburst (recurrence time, t_S), which seems to confirm the prediction by Osaki (1995), although t_{wait-S} is not strictly equal to t_S . On the other hand, superoutbursts after almost the same recurrence time showed somewhat different maximum magnitudes. The mass transfer rate can not be always regarded as constant.

Osaki (1995) also provided a model for WZ Sge-type dwarf novae which are a very inactive subgroup of SU UMa stars, and thought to be an end product of the CV evolution. Their model explained some of the observational properties of WZ Sge stars; for example, the extremely long recurrence time of superoutbursts (1000-10000 days), no (or few) normal outbursts, and the large amplitude of superoutbursts (6-8 mag). According to Osaki (1995), for dwarf novae with a moderately low mass

transfer rate, the recurrence time of the normal outbursts, t_N , is proportional to the inverse square of \dot{M} , and t_{wait-S} is proportional to the inverse of \dot{M} . They presented the number of outbursts in one supercycle as

$$\text{the number of normal outbursts} \propto t_{wait-S}/t_N \propto \dot{M}, \quad (7)$$

provided that $t_{wait-S} > t_N$. They suggested that if the mass transfer rate further decreases, we have $t_{wait-S} < t_N$. Then every normal outburst triggers a superoutburst; this case corresponds to WZ Sge stars. In SW UMa, the recurrence times of superoutbursts are about 400 to 1500 days, and these are somewhat shorter compared with WZ Sge stars (for example, about 30 years for WZ Sge itself). However, there is no (or few) normal outbursts in SW UMa, like WZ Sge stars. Therefore, this object has a relatively small mass transfer rate corresponding to $t_{wait-S} \sim t_N$, and it is going to evolve into WZ Sge type. The short orbital period of SW UMa is also consistent with the conclusion. This is also applicable in some SU UMa-type dwarf novae, e.g. WX Cet (Sterken et al. 2007) and BC UMa (Maehara et al. 2007).

4.2. Superhump Evolution

We will compare the superhump evolution during well observed superoutbursts of SW UMa, the 2000, the 2002, the 2006, and the 1996 superoutbursts. The delay time of appearance of the superhumps after the onset of the superoutburst was somewhat different in these four superoutbursts: the delay was about 4 days for the 2000 one (maximum magnitude, $m_{max} = 10.4$), 2 days for the 2002 one ($m_{max} = 10.5$), 6 days for the 2006 one ($m_{max} = 10.3$), and 4 days for the 1996 one ($m_{max} = 9.7$, Nogami et al. 1998). Lubow (1991) showed that the growth rate of the 3:1 resonance is proportional to q^2 (mass ratio $q = M_2/M_1$, where M_1 and M_2 are the masses of the primary white dwarf and the secondary star, respectively). This can not explain the variation of the delay time in the same object, however. Osaki & Meyer (2003), on the other hand, proposed that the suppression of the 3:1 resonance by the 2:1 resonance is the main cause of the long delay time in superoutbursts of WZ Sge stars. As mentioned by Kato et al. (2008), this interpretation predicts the variation of the delay time in the same object with a quite low mass ratio depending on the maximum radius of the accretion disk at the onset of superoutbursts. They also suggested that the suppression by the 2:1 resonance seems the cause of the variation of the delay time in SW UMa. The superoutbursts of SW UMa we investigated seems to agree with the trend suggested by Kato et al. (2008). Our investigation also indicates that the delay time was different, but the superhumps showed the same evolutionary trend after their appearance during these four superoutbursts as below.

During the 2000 superoutburst, after the appearance of the superhumps, the superhump amplitude reached the first maximum on HJD 2451592, gradually declined between HJD 2451593 and 2451600, then started to regrow, and finally reached the second maximum on HJD 2451602 (the left panel of figure 2). The $O - C$ dia-

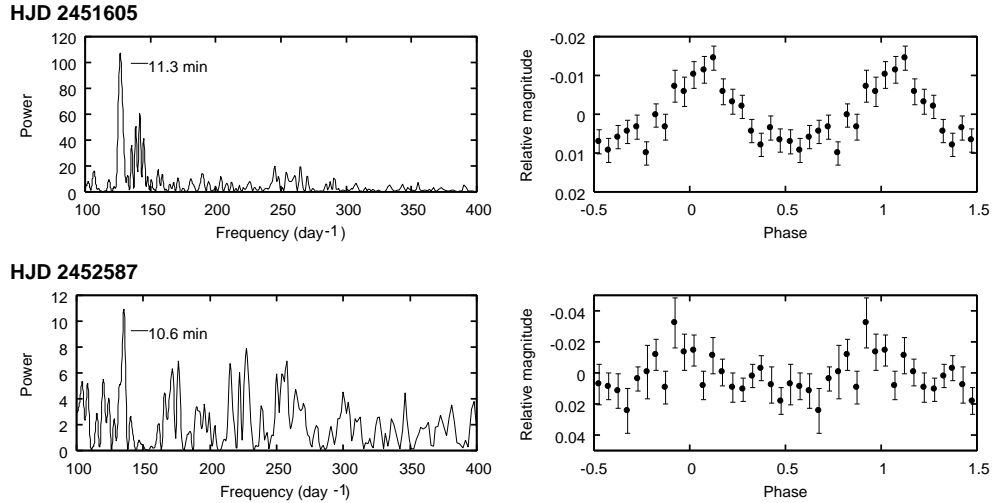


Fig. 19. Results of QPO analyses. The left and right panels are the power spectra and the phase-averaged light curves for each day at the end stage of the 2000, and the 2002 superoutbursts. The best estimated periods used in foldings are 11.3 min and 10.6 min in HJD 2451605 and 2452587, respectively.

gram on the maximum timings of the superhumps represents that the superhump period decreased around HJD 2451592, increased with the $P_{dot} = 7.1(3) \times 10^{-5}$ between HJD 2451592 and 2452602, and decreased again around HJD 2451602 (figure 4).

In the case of the 2002 superoutburst, although the first developing phase of the superhump was not observed well, the superhumps traced the same evolution as those during the 2000 one. The superhump period decreased around HJD 2452575 (probably the superhump amplitude reached the first maximum around here), and then increased with the $P_{dot} = 9.1(6) \times 10^{-5}$ from the first maximum until the second maximum of the superhump amplitude (between HJD 2452575 and 2452584). Successively, it decreased again around HJD 2452584 (figure 9 and 11).

The second maximum of the superhump amplitude accompanying the decrease of the superhump period at the end of the bright plateau stage could not be found during the 2006 superoutburst, due to the lack of the observation (see also section 4.1). At the early and middle stage, however, the superhumps also showed the same trend as those during the 2000 superoutburst. The superhump period decreased around the time of the amplitude maximum, and it gradually increased thereafter with the $P_{dot} = 6.5(6) \times 10^{-5}$ (figure 14 and 16).

Further, there is a sign of the same evolution of the superhumps during the 1996 one, although it was observed only at the middle stage. The superhump period increased with the $P_{dot} = 8.9(1.0)$ days cycle⁻¹ while the superhump amplitude were decreasing, and the amplitude regrew at the end of the increase of the period (see figure 2 and 3 in Semeniuk et al. 1997).

After their appearance, the superhumps showed the same evolutionary trend during the 2000 and the 2002 superoutbursts. This evolution agrees with the phenomenological suggestion by Soejima et al. (2009): the increase of the superhump period accompanies the regrowth of the

amplitude, and during a superoutburst with a regrowth of the superhump amplitude, the superhump period decreases around the first maximum of the amplitude, successively gradually increases until the second maximum of the amplitude, and decreases again after that. Since the superhumps during the 2006 and the 1996 ones showed the increase of the period and some similarities with those during the 2000 and the 2002 ones, the suggestion on the superhump evolution by Soejima et al. (2009) also seems applicable to the superhumps during these two superoutbursts. This same trend of superhump evolution during these four superoutbursts indicates that superhump evolution may be governed by invariable binary parameters, such as the mass ratio, the orbital period, and so on.

However, if the superhump evolution is different in superoutbursts of the same object, it is suggested to be affected by the variable features, e.g., the recurrence time of the outburst¹. As described above, the superhumps showed an increase of their period during all well observed superoutbursts of SW UMa. Kato et al. (1998) suggested that the outward propagation of the eccentricity generated at the 3:1 resonance radius leads to the increase of the superhump period. This predicts that, if the accretion disk does not expand sufficiently beyond the 3:1 resonance, the eccentricity can not propagate outward, and the superhump period can not increase. Since the superhumps showed a period increase, the accretion disk seemed to expand enough in the superoutbursts of SW UMa we investigated. These superoutbursts took place more than 500 days after the preceding superoutburst (table 8 and figure 18). It may be possible, however, that superoutbursts occur with a minimum recurrence time of ~ 400

¹ Although Uemura et al. (2005) found a difference of the derivative of the superhump period between during the 2001 and the 2004 superoutbursts of TV Crv, Kato et al. (in prep.) reanalysed the data, and suggest that the interpretation by Uemura et al. (2005) could not be confirmed.

days before sufficient mass is accumulated in the accretion disk. If different superhump evolutions are observed in different superoutbursts of one object, this will be a key to reveal which binary parameters govern the superhump evolution. Therefore, observation are required on superoutbursts of SW UMa which take place after shorter recurrence time in the future.

Detailed analyses have been also carried out in a few other SU UMa-type dwarf novae repeatedly during different superoutbursts; e.g., the 1989 one (O’Donoghue et al. 1991), the 1998 one (Kato et al. 2001a, Howell et al. 2002), the 2001 and the 2004 ones (Sterken et al. 2007) for WX Cet, the 2002 May and the 2006 ones for V844 Her (Oizumi et al. 2007), the 1992 one (Kato et al. 2001b) and the 2002 one (Ishioaka et al. 2003) for HV Vir. However, there is also a need for investigations on various superoutbursts of each object such as SW UMa, since clear differences of the superhump evolution have not been found.

4.3. Humps After Superoutbursts

After the rapid decline phase of superoutbursts, some SU UMa-type dwarf novae show periodic modulations with the ordinary superhump period, but the phase is shifted by typically ~ 0.5 . This phenomenon is called ‘late superhumps’ (Haefner et al 1979, Vogt 1983, van der Woerd et al. 1988).

In the light curves of the 2002 superoutburst of SW UMa, the superhumps seem to have two peaks (the primary peaks, and the secondary peaks are indicated by solid arrows and dashed arrows, respectively in figure 9). At the beginning, the primary humps were prominent, and the secondary humps progressively increased their amplitude at the end stage of the superoutburst. Such growth of secondary humps were also observed in SW UMa during the 1986 superoutbursts (Robinson et al. 1987), the 1991 one (Kato et al. 1992), the 1996 one (Semeniuk et al. 1997), and the 2000 one (this paper), and in addition, during superoutbursts of other objects (e.g. Schoembs & Vogt 1980, Udalski 1990). Schoembs & Vogt (1980) and Warner (1995) suggested that such secondary humps develop into late superhumps. If secondary humps replace the primary during the end stage of the superoutburst, and these humps have been regarded as late superhumps, it is naturally explained that late superhumps have shown the same period as that of the ordinary superhumps and the shifted phase in previous works.

We observed humps on HJD 2451606, at the end of the rapid decline phase of the 2000 superoutburst of SW UMa (figure 2). Although no hump was clearly visible after HJD 2451606, we obtained a periodicity of 0.05798 days from the data between HJD 2451607 and 2451610. This period is close to the superhump period at the end stage of the outburst (0.05771 days), between HJD 2451603 and 2451606. However, no obvious phase shift of ~ 0.5 was observed (figure 7). Humps after the rapid decline phase of the 2000 superoutburst, therefore, seems not late superhumps, but the remains of the ordinary superhumps.

4.4. QPOs

Quasi-Periodic Oscillations (QPOs) are observed in light curves of CVs and in X-ray binaries (see e.g. Warner & Woudt 2008). The typical amplitude and period are ~ 0.01 mag and ~ 300 s, respectively, for CVs. In SW UMa, Robinson et al. (1987) observed QPOs which had a amplitude of up to ~ 0.01 mag and a period of ~ 4.8 min during the 1986 superoutburst. Following this, as mentioned in section 1, Kato et al. (1992) discovered unusually large-amplitude QPOs (~ 0.2 mag) with a period of ~ 6.1 min during the 1992 superoutburst, and called them ‘super-QPOs’. Although Warner et al. (2003) also observed large QPOs with an amplitude of ~ 0.2 mag in quiescence of a dwarf nova, WX Hyi, such large QPOs are very rare in CVs. During the 1996 superoutburst of SW UMa, Nogami et al. (1998) found ordinary QPOs with an amplitude of ~ 0.01 mag and a period of ~ 5.3 min, but they failed to detect so-called ‘super-QPOs’.

We detected QPOs with an amplitude of ~ 0.02 mag at the end stage of the 2000 and the 2002 superoutbursts (figure 19), but could not find super-QPOs with such a large amplitude of ~ 0.2 mag. These QPOs we detected had a period of ~ 11 min, which is about twice as long as those detected at the early or middle stage of superoutbursts of SW UMa in previous works. QPOs with a similar period detected at the similar phase of two outbursts in our data indicate that these QPOs might have the same origin.

5. CONCLUSION

Our main conclusion in this paper is summarized below:

1. We investigated superhump evolutions during the 2000, the 2002, and the 2006 superoutbursts. After their appearance, the superhumps showed the same evolution during these superoutbursts, which implies that the superhump evolution may be governed by the invariable binary parameters, such as the mass ratio, the orbital period, and so on.
2. After the end of the 2000 superoutburst, we detected a periodicity close to the superhump in the light curve, but the phase shift which commonly accompanies late superhumps was not found.
3. We found QPOs at the end stage of the 2000 and the 2002 superoutbursts, but failed to detect so-called ‘super-QPOs’ during three superoutbursts we investigated.

We are grateful to many observers who have reported vital observations. We acknowledge with thanks the variable star observations from VSNET, AAVSO, and AFOEV International Database contributed by observers worldwide and used in this research.

This work was supported by the Grant-in-Aid for the Global COE Program “The Next Generation of Physics, Spun from Universality and Emergence” from the Ministry of Education, Culture, Sports, Science and Technology (MEXT) of Japan.

References

- Cannon Smith, R. 2007, astro-ph/071654
- Haefner, R., Schoembs, R., & Vogt, N. 1979, *A&A*, 77, 7
- Hellier, C. 2001, *Cataclysmic Variable Stars* (PublisherSpringer)
- Howell, S., & Szkody, P. 1988, *PASP*, 100, 224
- Howell, S. B., Szkody, P., Sonneborn, G., Fried, R., Mattei, J., Oliverson, R. J., Ingram, D., & Hurst, G. M. 1995, *ApJ*, 453, 454
- Howell, S. B., Fried, R., Szkody, P., Sirk, M. M., & Schmidt, G. 2002, *PASP*, 114, 748
- Ishioaka, R., et al 2003, *PASJ*, 55, 683
- Kato, T., Hirata, R., & Mineshige, S. 1992, *PASJ*, 44, 215
- Kato, T. 1995, *Inf. Bull. Variable Stars*, 4256
- Kato, T., Nogami, D., Baba, H., & Matsumoto, K. 1998, in *ASPConf. Ser. 137, Wild Stars in the Old West*, ed. S. Howell, E. Kuulkers, & C. Woodward (San Francisco: ASP), 9
- Kato, T., Matsumoto, K., Nogami, D., Morikawa, K., & Kiyota, S. 2001a, *PASJ*, 53, 893
- Kato, T., Sekine, Y., & Hirata, R. 2001b, *PASJ*, 53, 1191
- Kato, T., Nogami, D., Matsumoto, K., & Baba, H. 2004a, *PASJ*, 56, S109
- Kato, T., Maehara, H., & Monard, B. 2008, *PASJ*, 60, 23
- Lubow, S., H. 1991, *ApJ*, 381, 259
- Maehara, H., Hachisu, I., & Nakajima, K. 2007, *PASJ*, 59, 227
- Nogami, D., Kato, T., Baba, H., Matsumoto, K., Arimoto, J., Tanabe, K., & Ishikawa, K. 1997, *ApJ*, 490, 840
- Nogami, D., Baba, H., Kato, T., & Novák, R. 1998, *PASJ*, 50, 297
- O'Donoghue, D., Chen, A., Marang, F., Mittaz, J. P. D., Winkler, H., & Warner, B. 1991, *MNRAS*, 250, 363
- Oizumi et al. 2007, *PASJ*, 59, 643
- Olech, A., Schwarzenberg-Czerny, A., Kędzierski, P., Złoczewski, K., and Mularczyk, K., & Wiśniewski, M. 2003, *Acta Astron.*, 53, 175
- Olech, A., Cook, L. M., Złoczewski, K., Mularczyk, K., Kędzierski, P., Udalski, A., & Wiśniewski, M. 2004, *Acta Astron.*, 54, 2330
- Osaki, Y. 1974, *PASJ*, 26, 420
- Osaki, Y. 1989, *PASJ*, 41, 1005
- Osaki, Y. 1995, *PASJ*, 47, 47
- Osaki, Y., & Meyer, F. 2003, *A&A*, 401, 325
- Patterson, J., et al. 1998, *PASP*, 110, 1290
- Pavlenko, E. P., Shugarov, S. Yu., & Katysheva, N. A. 2000, *Ap*, 43, 419
- Robinson, E. L., Shafter, A. W., Hill, J. A., Wood, M. A., & Mattei, J. A. 1987, *ApJ*, 313, 772
- Schoembs, R., & Vogt, N. 1980, *A&A*, 91, 25
- Semiuk, I., Olech, A., Kwast, T., & Nalezyty, M. 1997, *Acta Astron.*, 47, 201
- Shafter, A. W., Szkody, P., & Thorstensen, J. R. 1986, *ApJ*, 308, 765
- Smak, J. 1985, *Acta Astron.*, 35, 351
- Smith, A. J., Haswell, C. A., Murray, J. R., Truss, M. R., & Foulkes, S. B. 2007, *MNRAS*, 378, 7855
- Soejima, Y., Imada, A., Nogami, D., Kato, T., & Berto Monard, L. A. G. 2009, *PASJ*, in press (arXiv:0812.3271)
- Stellingwerf, R. F. 1978, *ApJ*, 224, 953
- Sterken, C., Vogt, N., Schreiber, M. R., Uemura, M., & Tuvikene, T. 2007, *A&A*, 463, 1053
- Szkody, P., & Mattei, J. A. 1984, *PASP*, 96, 988
- Szkody, P., Stablein, C., Mattei, J. A., & Waagen, E. O. 1991, *ApJS*, 76, 359
- Udalski, A. 1990, *AJ*, 100, 226
- Uemura, M., et al. 2005, *A&A*, 432, 261
- van der Woerd, H., & van Paradijs, J. 1987, *MNRAS*, 224, 271
- van der Woerd, H., van der Klis, M., van Paradijs, J., Beuermann, K., & Motch, C. 1988, *ApJ*, 330, 911
- Vogt, N. 1983, *A&A*, 118, 95
- Warner, B. 1995, *Cataclysmic Variable Stars* (Cambridge University Press)
- Warner, B., Woudt, P. A., & Pretorius, M. L. 2003, *MNRAS*, 344, 1193
- Warner, B., & Woudt, P. A. 2008, *AIPC*, 1054, 101
- Wenzel, W., & Richter, G. A. 1986, *Astron. Nachr.*, 307, 209
- Whitehurst, R. 1994, *MNRAS*, 266, 35